

1 **Impact of grids and dynamical cores in CESM2.2 on**
2 **the meteorology and climate of the Arctic**

3 **Adam R. Herrington** ¹, **Marcus Lofverstrom** ², **Peter H. Lauritzen** ¹ and
4 **Andrew Gettelman** ¹

5 ¹National Center for Atmospheric Research, 1850 Table Mesa Drive, Boulder, Colorado, USA
6 ²Department of Geosciences, University of Arizona, 1040 E. 4th Street, Tucson, AZ USA

7 **Key Points:**

- 8 • enter point 1 here
9 • enter point 2 here
10 • enter point 3 here

Abstract

[enter your Abstract here]

Plain Language Summary

[enter your Plain Language Summary here or delete this section]

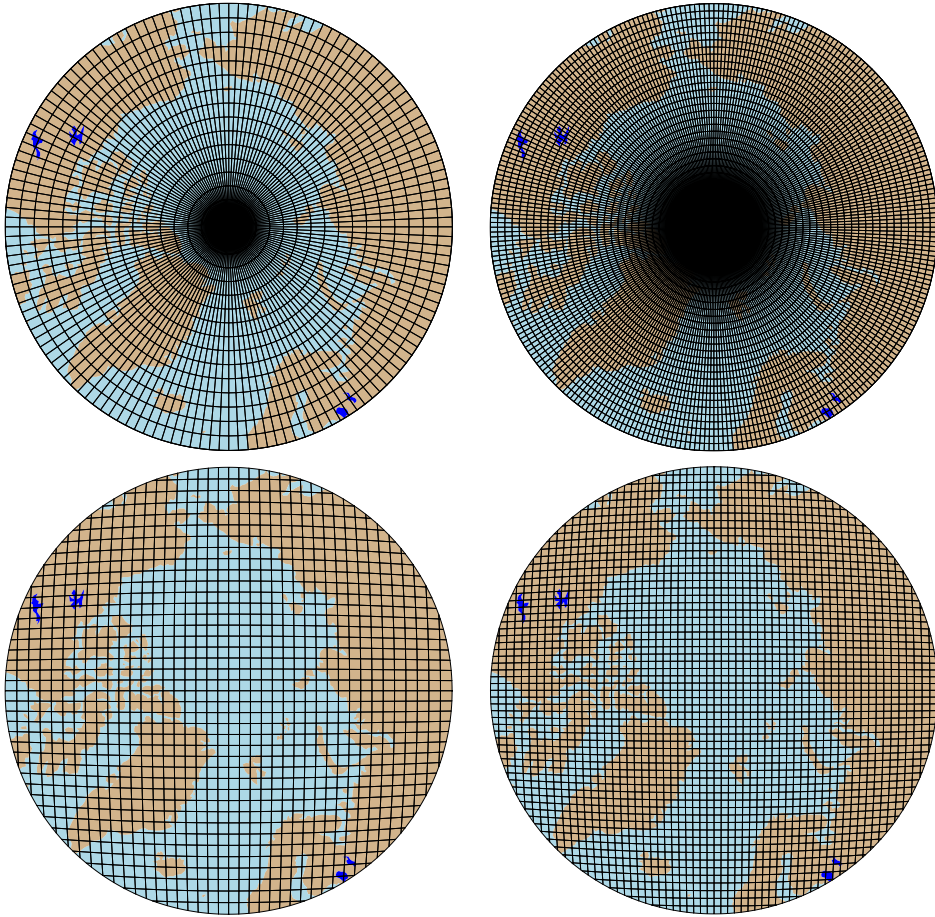
1 Introduction

General Circulation Models (GCMs) are powerful tools for understanding the meteorology and climate of the high-latitudes, which are among the most sensitive regions on Earth to global and environmental change. Despite their importance, the numerical treatment of polar regions is handled in vastly-different ways due to the so-called *pole-problem* (Williamson, 2007). The pole-problem refers to instability arising from the convergence of meridians at the polar points on latitude-longitude grids (e.g., Figure 1a). Depending on the numerics, methods exist to stabilize the pole problem, and latitude-longitude grids may be advantageous for polar processes as structures can be represented with more degrees of freedom than elsewhere in the computational domain. With the recent trend towards globally uniform unstructured grids, any potential benefits of latitude-longitude grids on polar regions may become a relic of the past. In this study, a spectrum of grids and dynamical cores (hereafter referred to as *dycores*) available in the Community Earth System Model, version 2.2 (CESM; <http://www.cesm.ucar.edu/models/cesm2/>), from conventional latitude-longitude grids to unstructured grids with globally uniform grid spacing to unstructured grids with regional refinement over the Arctic, are evaluated to understand their impacts on the simulated characteristics of the Arctic, with a special focus on the Greenland Ice Sheet.

In the 1970's the pole problem was largely defeated through wide-spread adoption of efficient spectral transform methods in GCMs. These methods transform grid point fields into a global, isotropic representation in wave space, where linear operators in the equation set can be solved for exactly. While spectral transform methods are still commonly used in the 21st century, local numerical methods have become desirable for their ability to run efficiently on massively parallel systems. The pole-problem has thus re-emerged in contemporary climate models that use latitude-longitude grids, and some combination of reduced grids and polar filters are necessary to ameliorate this instability (Jablonowski & Williamson, 2011). Polar filters are akin to a band-aid; they subdue the growth of unstable modes by applying additional damping to the solution over polar regions. One might expect that this additional damping reduces the effective resolution such that the resolved scales are similar across the entire domain, but this seems an unlikely outcome and is explored further in this study.

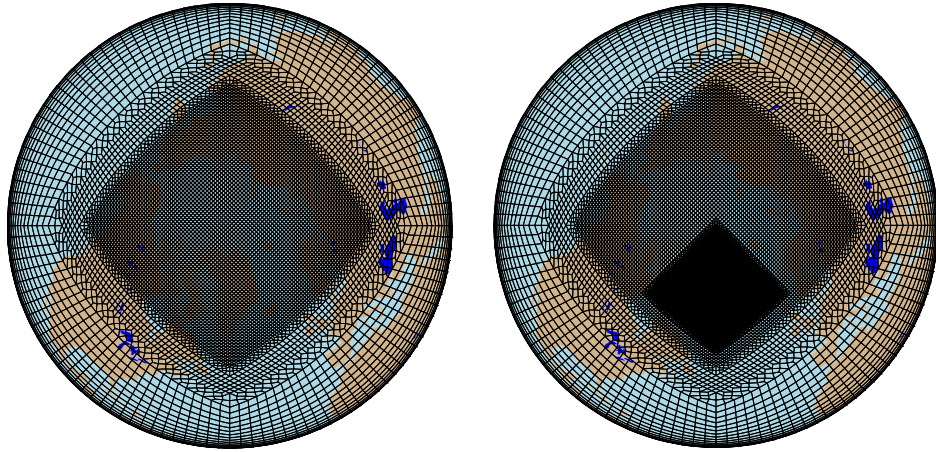
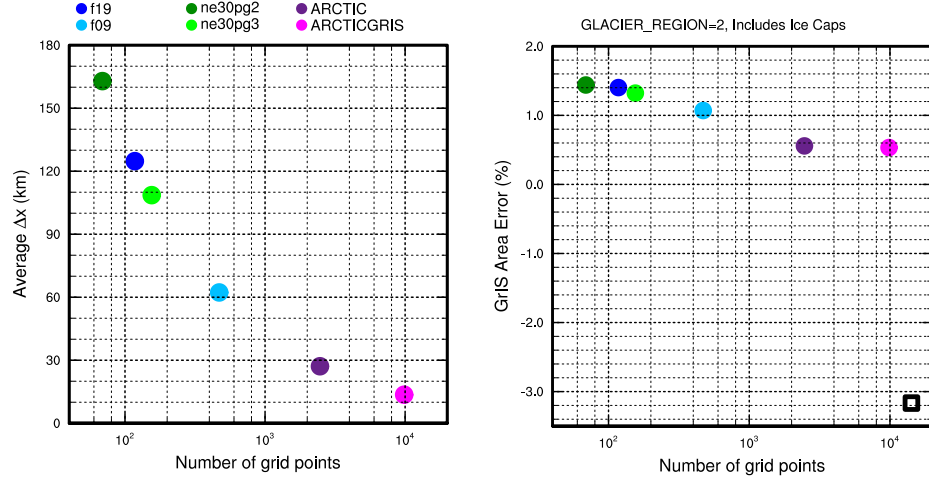
An alternative approach is to use unstructured grids. Unstructured grids allow for more flexible grid structures, permitting quasi-uniform grid spacing globally that eliminates the pole-problem entirely (e.g., Figure 1c). This grid flexibility also allows for variable-resolution or regional grid refinement. Grids can be developed with refinement over polar regions that could in principle make up for any loss in polar resolution in transitioning away from latitude-longitude grids (e.g., Figure 2), although this comes at the cost of a smaller CFL-limiting time-step in the refined region. But unstructured grids scale more efficiently on parallel systems than latitude-longitude grids, resulting in latitude-longitude grids becoming less common, and unstructured grids more common as computing power continued to increase over time.

The meteorology and climate of the Arctic is characterized by a range of processes and scales that are difficult to represent in GCMs (Bromwich et al., 2001; Smirnova & Golubkin, 2017; van Kampenhout et al., 2018). Synoptic scale storms are well represented

**Figure 1.** .

at typical GCM resolutions, but mesoscale Polar Lows are not. These mesoscale systems are prevalent during the cold season, and produce gale-force winds that can induce large fluxes through the underlying sea-ice/ocean interface. The Arctic also contains the Greenland Ice Sheet (hereafter denoted as *GrIS*). While it blankets the largest island in the world (Greenland), *GrIS* is only marginally resolved at typical GCM resolutions. *GrIS* ablation zones exert a primary control on the mass balance of the ice sheet, but are on the order of 100km wide, and models struggle to resolve these narrow features. *GrIS* elevations descend rapidly toward the coasts, resulting in steep margins that facilitate orographic precipitation events, but which are not well resolved in GCMs. The Arctic is therefore well-suited to understand the impact of different grids and dycores on processes that are marginally resolved at conventional GCM resolutions.

The goal of this study is to characterize the representation of high-latitude regions using the spectral-element and finite-volume dycores in CESM2.2, as these models treat the high-latitudes, e.g., the pole-problem, in very different ways. The manuscript is laid out as follows. Section 2 consists of documentation of the grids, dycores and physical parameterizations used in this study. The Arctic refined grids were developed by the authors, and this section serves as their official documentation in CESM2.2. Section 2 also contains a description of the experiments along with the observational datasets and post-processing software used for evaluating the models. Section 3 contains the results of the experiments and Section 4 provides some discussion and conclusions.

**Figure 2.****Figure 3.**

79 2 Methods

80 2.1 Grids and dynamical cores

81 The atmospheric component of CESM2.2, the Community Atmosphere Model, ver-
 82 sion 6.3 (CAM; <https://ncar.github.io/CAM/doc/build/html/index.html>), supports
 83 a diverse number of atmospheric dynamical cores. These range from dycores using latitude-
 84 longitude grids, the finite-volume (FV; Lin, 2004) and eulerian spectral transform (EUL;
 85 Collins et al., 2006) models, and dycores built on unstructured grids, the spectral-element
 86 (SE; Lauritzen et al., 2018) and finite-volume 3 (FV3; Putman & Lin, 2007) models. The
 87 EUL dycore is the oldest dycore in CAM, and the least supported of all the dycores in
 88 the current model. FV3 is the newest dycore in CAM, but it was not fully incorporated
 89 at the time this work commenced, and so is omitted from this study. The authors in-
 stead focus on the two most well supported dycores in CAM, SE and FV.

91 **2.1.1 Finite-volume model**

92 The FV dycore is a hydrostatic model that integrates the equations of motion using
 93 a finite-volume discretization on a global latitude-longitude grid. The 2D dynamics
 94 evolve in floating Lagrangian layers that are periodically mapped to Eulerian refer-
 95 ence grid in the vertical. Hyperviscous damping is applied to the divergent modes while
 96 Laplacian damping is applied to momentum in the top few layers, referred to as a “sponge
 97 layer.” A polar filter is used to avoid computational instability due to the convergence
 98 of the meridians, permitting the use of a more practical time-step. It takes the form of
 99 a Fourier filter in the zonal direction, with the damping coefficients increasing monoton-
 100 ically poleward. The FV dycore is run with grids Δx of 1° and 2° grid spacing, referred
 101 to as f09 and f19, respectively (Figure 1a,b).

102 **2.1.2 Spectral-element model**

103 The SE dycore is a hydrostatic model that integrates the equations of motion using
 104 a high-order continuous Galerkin method. The computational domain is defined by
 105 a cubed-sphere grid that is tiled with quasi-equal area quadrilateral elements (e.g., Fig-
 106 ure 2). Each element contains a fourth order basis set in the two horizontal directions,
 107 and the solution defined at the roots of the basis functions, the Gauss-Lobatto-Lagendre
 108 (GLL) quadrature points. This results in 16 GLL point values within each element, with
 109 12 of the points lying on the element boundary. This compact support allows for effi-
 110 cient parallelization up to one element for task. Communication between elements hap-
 111 pens via the direct stiffness summation, which applies a numerical flux to the element
 112 boundaries to reconcile overlapping nodal point values, and resulting in a continuous global
 113 basis set.

114 As with the FV dycore, the dynamics evolve in floating Lagrangian layers that are
 115 subsequently mapped to a Eulerian reference grid. The 2D dynamics have no implicit
 116 dissipation and so hyperviscosity operators are applied to all prognostic variables to re-
 117 move spurious numerical errors. Laplacian damping is applied in the sponge layer, sim-
 118 ilar to the FV dycore.

119 The SE dycore supports regional grid refinement via its variable-resolution config-
 120 uration. Two variable resolution meshes were developed as part of the CESM2.2 release
 121 that contains grid refinement over the Arctic. The software package SQuadgen (<https://github.com/ClimateGlobalChange/squadgen>) was used to generate these meshes. The
 122 ARCTIC grid is a $\Delta x = 1^\circ$ grid with $\Delta x = \frac{1}{4}^\circ$ regional refinement over the broader
 123 Arctic region. The ARCTICGRIS grid is similar to the ARCTIC grid, but addition-
 124 ally contains a patch covering the big island of Greenland with $\Delta x = \frac{1}{8}^\circ$ resolution. Both
 125 grids are depicted in Figure 2.

126 For spectral-element grids with quasi-uniform grid spacing, a variant in which tracer
 127 advection is computed using the Conservative Semi-Lagrangian Mult-tracer tranport
 128 scheme is used instead (Lauritzen et al., 2017, CSLAM). CSLAM has improved tracer
 129 property preservation and accelerated multi-tracer transport. It uses a seperate grid from
 130 the spectral-element dynamics, through dividing each element into 3×3 quasi-equal area
 131 control volumes. The physical parameterizations are computed from the state on the CSLAM
 132 grid, which has clear advantages over the default SE dycore in which the physics are eval-
 133 uated at the GLL nodal points (A. Herrington et al., 2018).

134 The 1° CAM-SE-CSLAM grid is referred to as ne30pg3 (Figure 1c). The *ne* indicates
 135 the number of elements along an edge of a cubed-sphere face, and the *pg* denotes
 136 the number of control volumes along the edge of an element used for computing the phys-
 137 ical parameterizations. Optionally, one can compute the physics on a finite-volume grid
 138 that is $\frac{3}{2} \times \Delta x$ of the tracer-advection grid, found through dividing the elmenet into $2 \times$
 139 2 control volumes (A. R. Herrington et al., 2019, (Figure 1d)). A comparison of this lower-

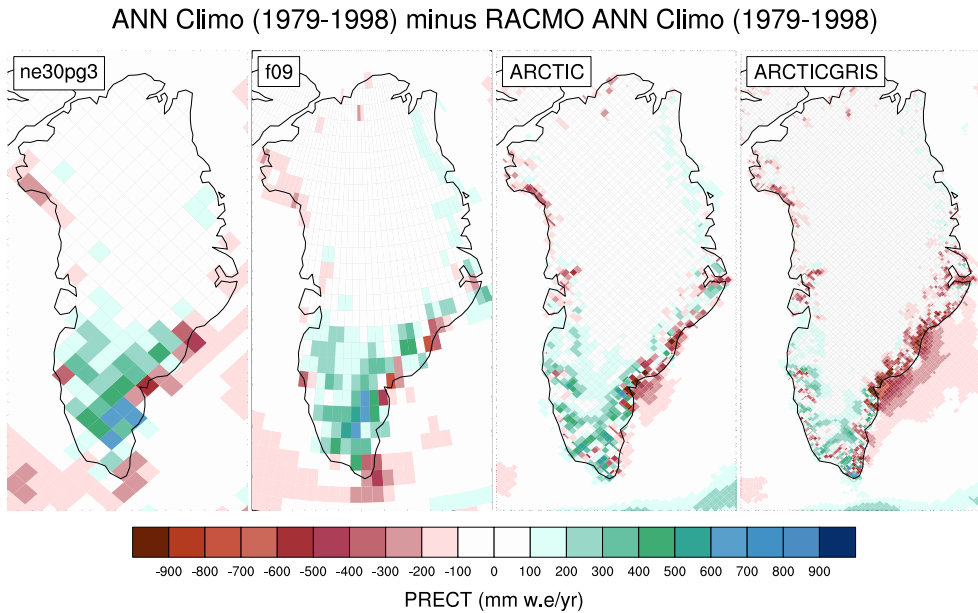
141 resolution physics grid *ne30pg2* over the Arctic is included in this study. All variants of
 142 the SE dycore discussed herein are available as part of the CESM2.2 release.

143 2.2 Physical parameterizations

144 The CAM6 physical parameterization package (hereafter referred to as the *physics*;
 145 <https://ncar.github.io/CAM/doc/build/html/index.html>) is used for all simula-
 146 tions in this study. CAM6 physics is most notably different from its predecessors through
 147 the incorporation of high-order turbulence closure, Cloud Layers Unified by Binormals
 148 (Golaz et al., 2002; Bogenschutz et al., 2013, CLUBB), which jointly acts as a PBL, shal-
 149 low convection and cloud macrophysics scheme. CLUBB is coupled with the MG2 mi-
 150 crophysics scheme (Gettelman et al., 2015), with prognostic precipitation and classical
 151 nucleation theory in representing cloud ice for improved cloud-aerosol interactions. Deep
 152 convection is parameterized using a convective quasi-equilibrium mass flux scheme (Zhang
 153 & McFarlane, 1995; Neale et al., 2008) including convective momentum transport (Richter
 154 et al., 2010). PBL form drag is modeled after (Beljaars et al., 2004) and orographic grav-
 155 ity wave drag is represented with an anisotropic method driven by the orientation of to-
 156 topographic ridges at the sub-grid scale.

157 2.3 Experimental design

158 All grids and dycores are run using an identical transient 1979-1998 AMIP-style
 159 configuration, with prescribed monthly SST/sea-ice after (Hurrell et al., 2008). This con-
 160 figuration refers to the *FHIST compset* and runs out of the box in CESM2.2. The Com-
 161 munity Land Model (CLM5; [https://escomp.github.io/clm5-docs/versions/release-
 162 -clm5.0/html/users_guide/index.html](https://escomp.github.io/clm5-docs/versions/release-clm5.0/html/users_guide/index.html)) calculates the surface energy balance at each
 163 land tile within a grid cell, which is used to compute snow and bare ice melting to in-
 164 form the surface mass balance (SMB) of a glacier unit (van Kampenhout et al., 2020).
 165 Ice accumulation is modeled as a capping flux, or snow in excess of the assumed 10 m
 166 snow cap, and refreezing of liquid within the snowpack additionally acts as a source of
 167 mass in the SMB calculation. The SMB of the GrIS was spun-up for the variable-resolution
 168 grids by forcing CLM5 offline, cycling over 20 years of a fully coupled *ARCTIC* run for
 169 about 500 years. The uniform resolution grids are all initialized with an SMB from an
 170 existing *f09* spun-up initial condition.

**Figure 4.**

171 **2.4 Observational datasets**

172 **2.4.1 ERA5**

173 **2.4.2 LIVVkit 2.1**

174 **2.5 TempestExtremes**

175 **2.6 StormCompositor**

176 **3 Results**

177 **3.1 Tropospheric temperatures**

178 **3.2 Inter-annual variability**

179 **3.3 Synoptic-scale storm characteristics**

180 **3.4 Orographic gravity waves emanating from Greenland**

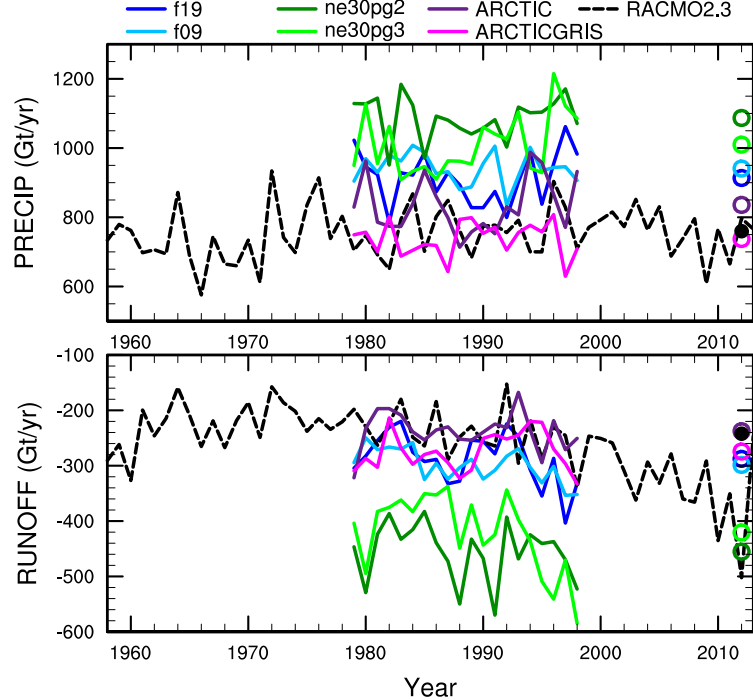
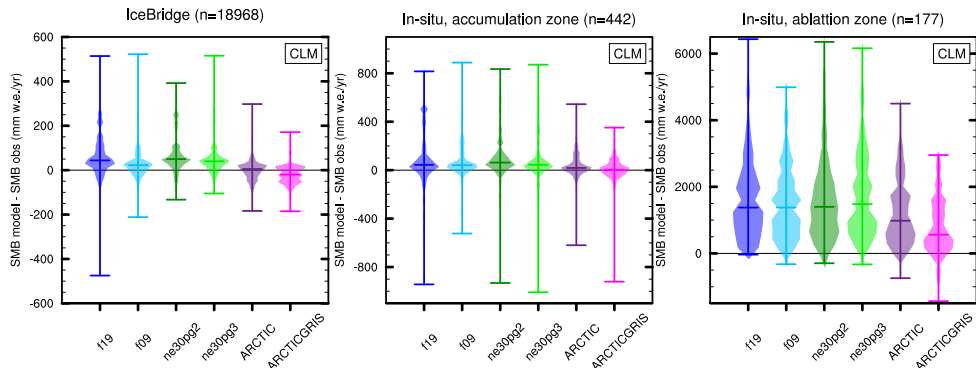
181 **3.5 Katabatic winds emanating from Greenland**

182 **3.6 Greenland surface mass balance**

183 **4 Conclusions**

184 **Acknowledgments**

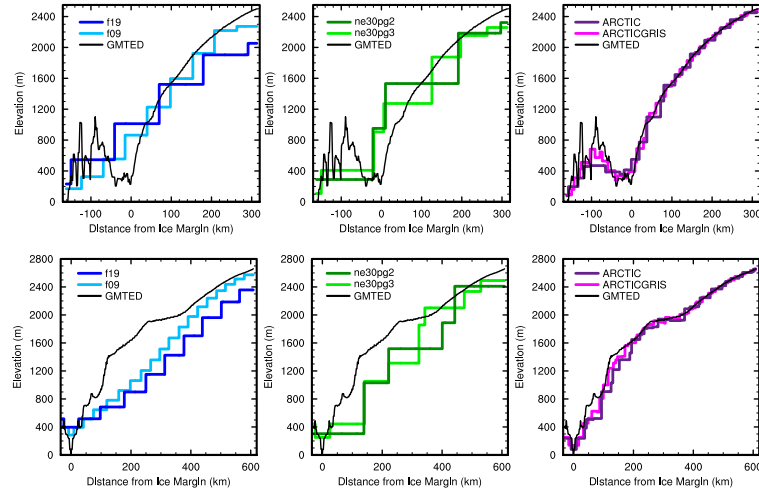
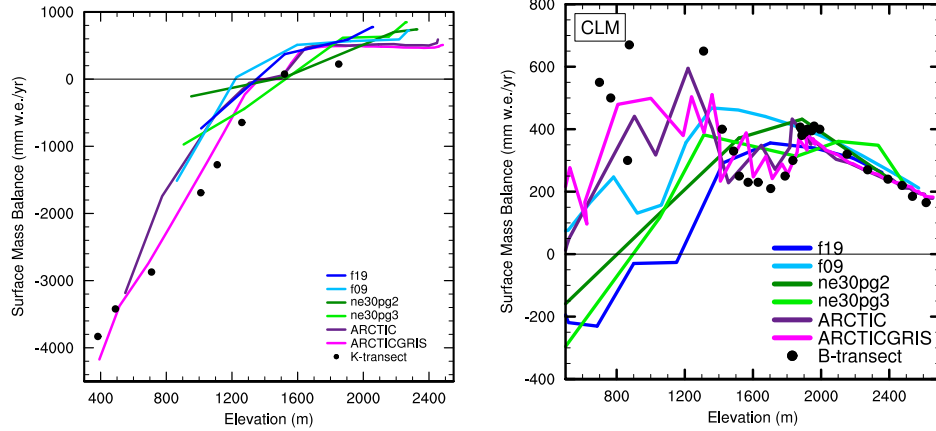
185 This material is based upon work supported by the National Center for Atmospheric Re-
 186 search (NCAR), which is a major facility sponsored by the NSF under Cooperative Agree-
 187 ment 1852977. Computing and data storage resources, including the Cheyenne super-
 188 computer (doi:10.5065/D6RX99HX), were provided by the Computational and Informa-
 189 tion Systems Laboratory (CISL) at NCAR.

**Figure 5.****Figure 6.**

190 The data presented in this manuscript is available at <https://github.com/adamrher/>
 191 2020-arcticgrids.

192 References

- 193 Beljaars, A., Brown, A., & Wood, N. (2004). A new parametrization of turbulent
 194 orographic form drag. *Quart. J. Roy. Meteor. Soc.*, *130*(599), 1327–1347. doi:
 195 10.1256/qj.03.73
- 196 Bogenschutz, P. A., Gettelman, A., Morrison, H., Larson, V. E., Craig, C., & Scha-
 197 nen, D. P. (2013). Higher-order turbulence closure and its impact on climate
 198 simulations in the community atmosphere model. *Journal of Climate*, *26*(23),
 199 9655–9676.

**Figure 7.** .**Figure 8.** .

- 200 Bromwich, D. H., Cassano, J. J., Klein, T., Heinemann, G., Hines, K. M., Steffen,
 201 K., & Box, J. E. (2001). Mesoscale modeling of katabatic winds over greenland
 202 with the polar mm5. *Monthly Weather Review*, 129(9), 2290–2309.
- 203 Collins, W. D., Rasch, P. J., Boville, B. A., Hack, J. J., McCaa, J. R., Williamson,
 204 D. L., ... Zhang, M. (2006). The formulation and atmospheric simulation
 205 of the community atmosphere model version 3 (cam3). *Journal of Climate*,
 206 19(11), 2144–2161.
- 207 Gettelman, A., Morrison, H., Santos, S., Bogenschutz, P., & Caldwell, P. (2015).
 208 Advanced two-moment bulk microphysics for global models. part ii: Global
 209 model solutions and aerosol–cloud interactions. *Journal of Climate*, 28(3),
 210 1288–1307.
- 211 Golaz, J.-C., Larson, V. E., & Cotton, W. R. (2002). A pdf-based model for bound-
 212 ary layer clouds. part i: Method and model description. *Journal of the Atmo-*
213 spheric Sciences, 59(24), 3540–3551. doi: 10.1175/1520-0469(2002)059<3540:
214 apbmfb>2.0.co;2
- 215 Herrington, A., Lauritzen, P., Taylor, M. A., Goldhaber, S., Eaton, B. E., Bacmeis-
 216 ter, J., ... Ullrich, P. (2018). Physics-dynamics coupling with element-based

- high-order galerkin methods: quasi equal-area physics grid. *Mon. Wea. Rev.*, 47, 69–84. doi: 10.1175/MWR-D-18-0136.1
- Herrington, A. R., Lauritzen, P. H., Reed, K. A., Goldhaber, S., & Eaton, B. E. (2019). Exploring a lower resolution physics grid in cam-se-cslam. *Journal of Advances in Modeling Earth Systems*, 11.
- Hurrell, J. W., Hack, J. J., Shea, D., Caron, J. M., & Rosinski, J. (2008). A new sea surface temperature and sea ice boundary dataset for the community atmosphere model. *Journal of Climate*, 21(19), 5145–5153.
- Jablonowski, C., & Williamson, D. L. (2011). The pros and cons of diffusion, filters and fixers in atmospheric general circulation models., in: P.H. Lauritzen, R.D. Nair, C. Jablonowski, M. Taylor (Eds.), Numerical techniques for global atmospheric models. *Lecture Notes in Computational Science and Engineering*, Springer, 80.
- Lauritzen, P. H., Nair, R., Herrington, A., Callaghan, P., Goldhaber, S., Dennis, J., ... Dubos, T. (2018). NCAR CESM2.0 release of CAM-SE: A reformulation of the spectral-element dynamical core in dry-mass vertical coordinates with comprehensive treatment of condensates and energy. *J. Adv. Model. Earth Syst.*. doi: 10.1029/2017MS001257
- Lauritzen, P. H., Taylor, M. A., Overfelt, J., Ullrich, P. A., Nair, R. D., Goldhaber, S., & Kelly, R. (2017). CAM-SE-CSLAM: Consistent coupling of a conservative semi-lagrangian finite-volume method with spectral element dynamics. *Mon. Wea. Rev.*, 145(3), 833-855. doi: 10.1175/MWR-D-16-0258.1
- Lin, S.-J. (2004). A 'vertically Lagrangian' finite-volume dynamical core for global models. *Mon. Wea. Rev.*, 132, 2293-2307.
- Neale, R. B., Richter, J. H., & Jochum, M. (2008). The impact of convection on ENSO: From a delayed oscillator to a series of events. *J. Climate*, 21, 5904-5924.
- Putman, W. M., & Lin, S.-J. (2007). Finite-volume transport on various cubed-sphere grids. *J. Comput. Phys.*, 227(1), 55-78.
- Richter, J. H., Sassi, F., & Garcia, R. R. (2010). Toward a physically based gravity wave source parameterization in a general circulation model. *J. Atmos. Sci.*, 67, 136-156. doi: dx.doi.org/10.1175/2009JAS3112.1
- Smirnova, J., & Golubkin, P. (2017). Comparing polar lows in atmospheric reanalyses: Arctic system reanalysis versus era-interim. *Monthly Weather Review*, 145(6), 2375–2383.
- van Kampenhout, L., Lenaerts, J. T., Lipscomb, W. H., Lhermitte, S., Noël, B., Vizcaíno, M., ... van den Broeke, M. R. (2020). Present-day greenland ice sheet climate and surface mass balance in cesm2. *Journal of Geophysical Research: Earth Surface*, 125(2), e2019JF005318.
- van Kampenhout, L., Rhoades, A. M., Herrington, A. R., Zarzycki, C. M., Lenaerts, J. T. M., Sacks, W. J., & van den Broeke, M. R. (2018). Regional grid refinement in an earth system model: Impacts on the simulated greenland surface mass balance. *The Cryosphere Discuss.*. doi: 10.5194/tc-2018-257
- Williamson, D. (2007). The evolution of dynamical cores for global atmospheric models. *J. Meteor. Soc. Japan*, 85, 241-269.
- Zhang, G., & McFarlane, N. (1995). Sensitivity of climate simulations to the parameterization of cumulus convection in the canadian climate centre general circulation model. *Atmosphere-ocean*, 33(3), 407-446.